SAND2019-7639C

Insights into spin-orbit coupling at the Si/SiO_2 interface using an inter-valley hot spot singlet/triplet qubit

Toby Jacobson[1], Ryan M. Jock[2], Martin Rudolph[2], Dan. R. Ward[2], Andrew D. Baczewski[1], Malcolm S. Carroll[2] and Dwight R. Luhman[2]

[1] Center for Computing Research, Sandia National Laboratories, Albuquerque, NM, USA

[2] Sandia National Laboratories, Albuquerque, NM, USA

Introduction

- When valley splitting and Zeeman splitting are in resonance, the well-known spin-valley "hot spot" results in an enhanced spin relaxation rate [1-4] for electrons confined to silicon quantum dots (QDs). While this spin-valley mechanism drives decoherence, it can also drive qubit rotations [5-8].
- Here, we demonstrate a S/T_0 qubit driven by intra- and inter-valley SOC. We have measured the frequency dependence of S/T_0 rotations near the hot spot for a thorough range of B-field orientations.
- We have extended a comprehensive intra-/inter-valley theory that captures the observed B-field dependence, in good agreement with the experiment.
- This technique allows for very precise measurement of valley splitting in this system, and may provide further insights into the nature of SOC at the Si/SiO_2 interface.

MOS DQD SO Driven S-T Qubits

Device Layout

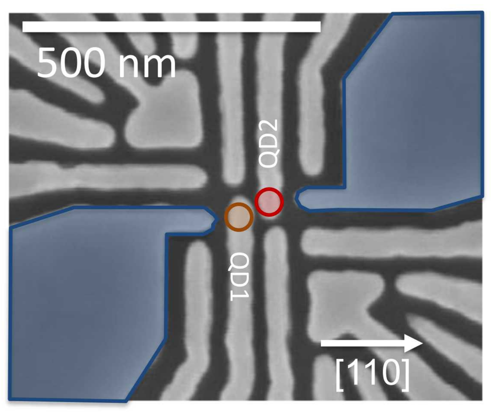

Charge Stability Diagram

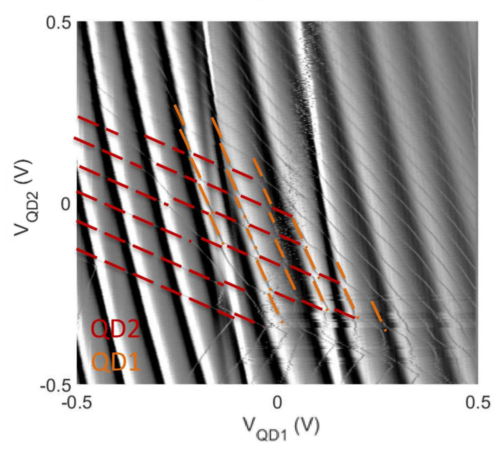

Singlet-Triplet FID

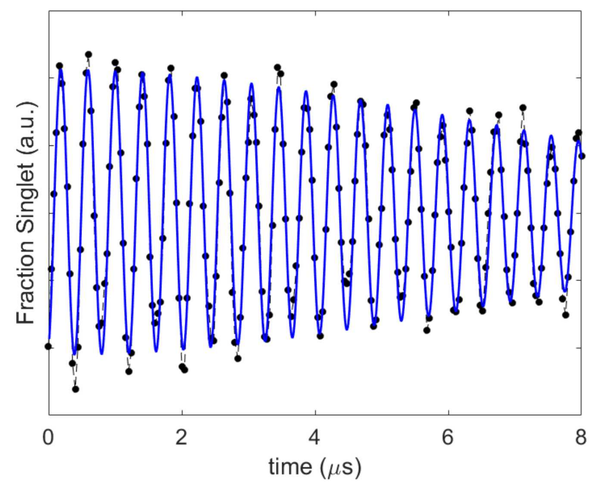

- Single poly-silicon gate layout
- 50nm gate oxide
- Isotopically enriched epi-layer with 500ppm residual ^{29}Si.
- Qubit Pair: (0,4)—(1,3) charge occupations on QD1 and QD2

Valley Hot-Spot Interaction

Model fits (red) superimposed on FFT of measured qubit rotation frequency as a function of B-field magnitude for 12 distinct B-field orientations. The full angular dependence is captured by the model

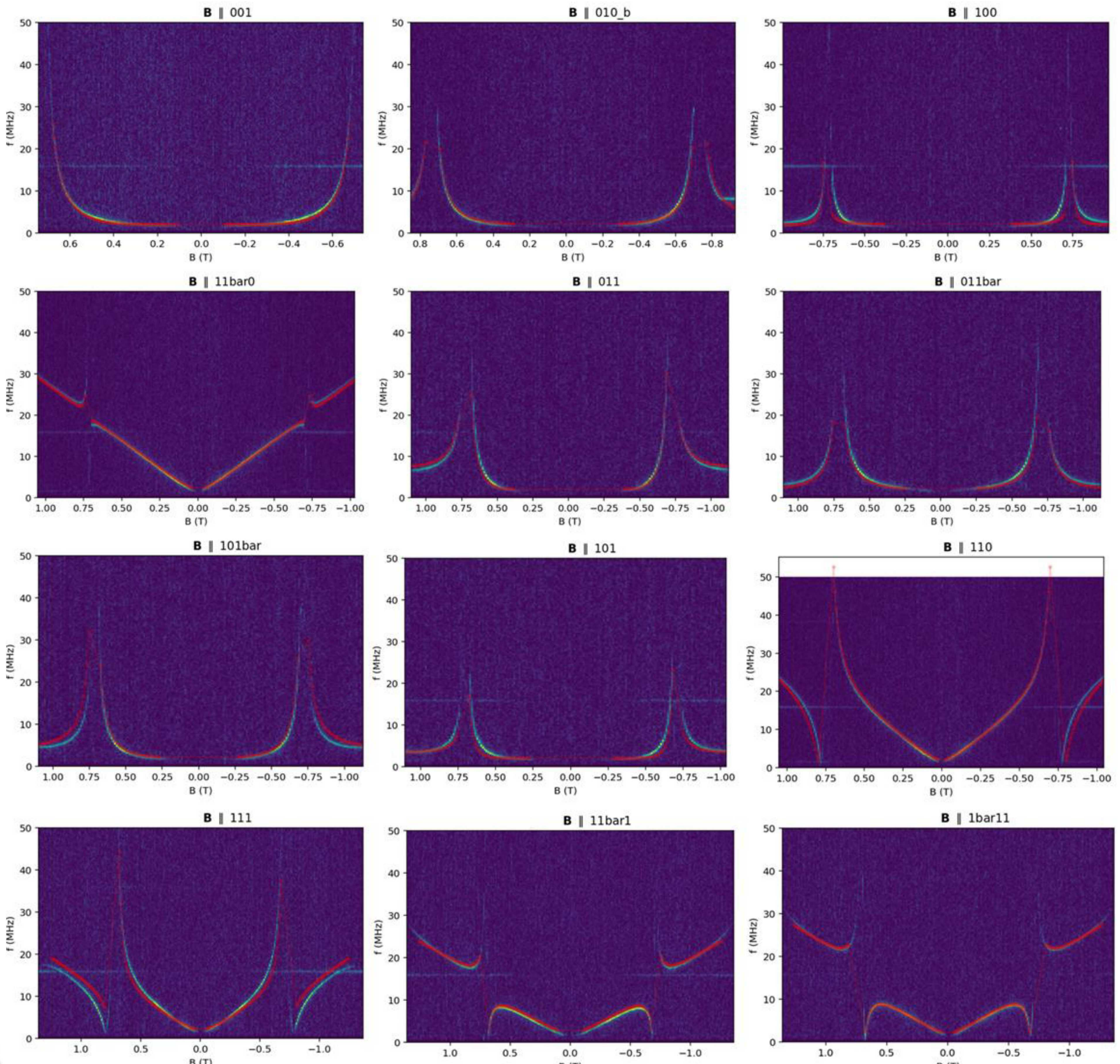

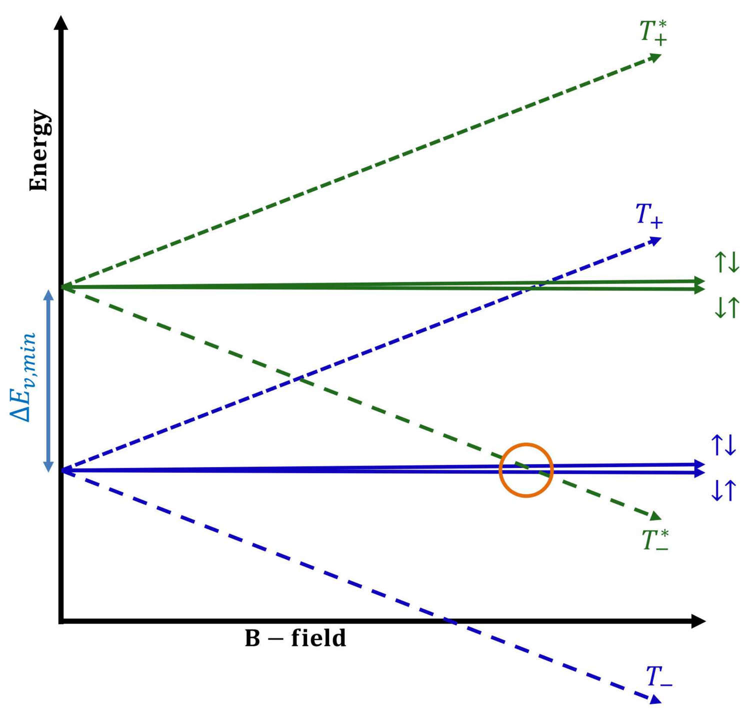

Hot spot Taxonomy

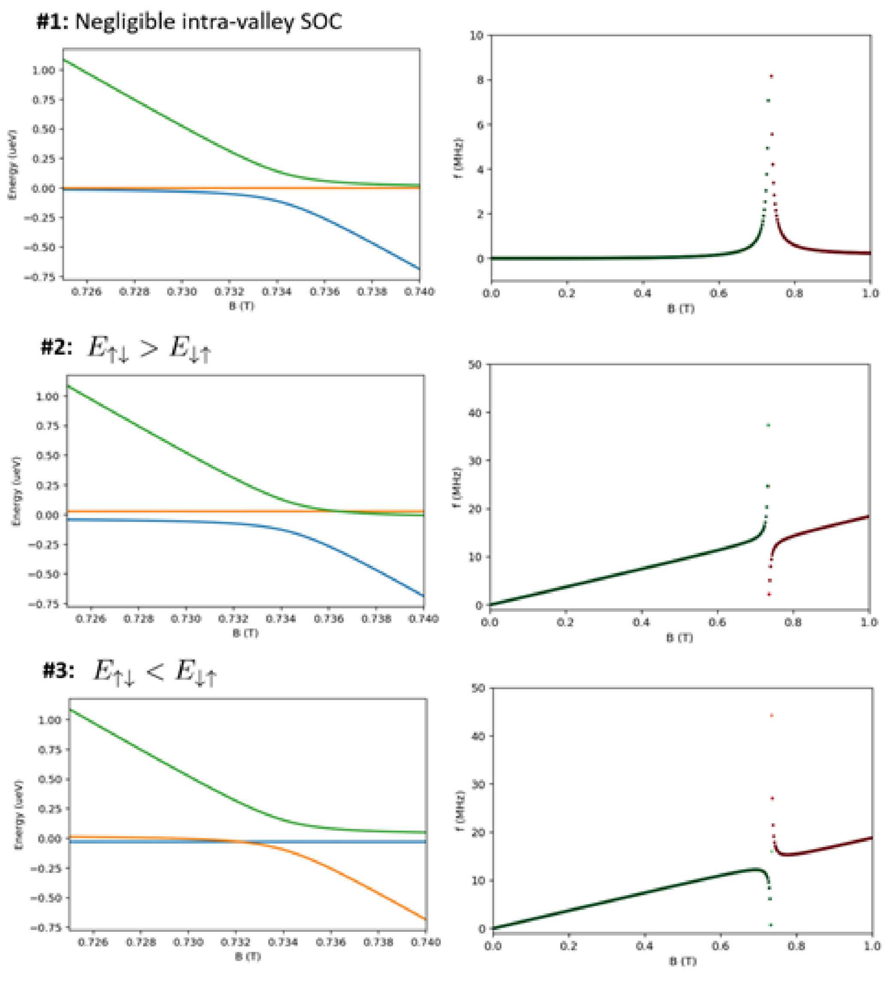

Effective Hamiltonian near the hot spot (for fixed B-field orientation)

$$H_{3\times3} = \begin{array}{c} \quad |S\rangle \qquad\quad |T_0\rangle \qquad\quad |T_-^*\rangle \\ \begin{pmatrix} 0 & B\delta & B\gamma e^{i\phi} \\ B\delta & 0 & -B\gamma e^{i\phi} \\ \gamma B e^{-i\phi} & -B\gamma e^{-i\phi} & \Delta_{\rm vs} - g\mu_B B \end{pmatrix} \end{array}$$

Depend strongly on orientation of **B** $\left\{ \begin{array}{l} \delta \text{ = intra-valley SOC strength} \\ \gamma \text{ = inter-valley SOC strength} \end{array} \right.$

$\Delta_{\rm vs}$ = valley splitting

Eigenenergy	Eigenstate
δB	$\frac{1}{\sqrt{2}}\begin{pmatrix}1\\1\\0\end{pmatrix}$
$\frac{1}{2}(\Delta_{\rm vs} - (\delta + g\mu_B)B) + \frac{1}{2}\sqrt{(\Delta_{\rm vs} + (\delta - g\mu_B)B)^2 + 8\gamma^2 B^2}$	$\frac{1}{\sqrt{2}}\begin{pmatrix}\frac{1}{2}e^{i\phi/2}w_-\\ -\frac{1}{2}e^{i\phi/2}w_-\\ \frac{1}{\sqrt{2}}e^{-i\phi/2}w_+\end{pmatrix}$
$\frac{1}{2}(\Delta_{\rm vs} - (\delta + g\mu_B)B) - \frac{1}{2}\sqrt{(\Delta_{\rm vs} + (\delta - g\mu_B)B)^2 + 8\gamma^2 B^2}$	$\frac{1}{\sqrt{2}}\begin{pmatrix}-\frac{1}{2}e^{i\phi/2}w_+\\ \frac{1}{2}e^{i\phi/2}w_+\\ \frac{1}{\sqrt{2}}e^{-i\phi/2}w_-\end{pmatrix}$

Intra-valley

$$\begin{aligned} \langle\tilde{S}|H|\tilde{T}_0\rangle &= \frac{1}{\sqrt{2}}\sin(\theta)\left(e^{i\varphi}\langle S|H|T_-\rangle - e^{-i\varphi}\langle S|H|T_+\rangle\right) \\ &= \frac{1}{2}\sin(\theta)\left[e^{i\varphi}\left(h^{LL}_{\uparrow\downarrow} - h^{RR}_{\uparrow\downarrow}\right) + e^{-i\varphi}\left(h^{LL}_{\downarrow\uparrow} - h^{RR}_{\downarrow\uparrow}\right)\right] \end{aligned}$$

Inter-valley

$$\begin{aligned} \langle\tilde{S}|H|\tilde{T}_-^*\rangle &= e^{-i\varphi}\sin^2\left(\frac{\theta}{2}\right)\langle S|H|T_+^*\rangle + e^{i\varphi}\cos^2\left(\frac{\theta}{2}\right)\langle S|H|T_-^*\rangle \\ &= \frac{1}{\sqrt{2}}\left(\sin^2\left(\frac{\theta}{2}\right)e^{-i\varphi}h^{RR^*}_{\downarrow\uparrow} - \cos^2\left(\frac{\theta}{2}\right)e^{i\varphi}h^{RR^*}_{\uparrow\downarrow}\right) \end{aligned}$$

$\langle\tilde{T}_0|H|\tilde{T}_-^*\rangle = -\langle\tilde{S}|H|\tilde{T}_-^*\rangle$ (reason for special structure of 3x3 Hamiltonian)

where $h^{MN}_{s_1 s_2} \equiv \langle\phi_M s_1|H_{\rm SO}|\phi_N s_2\rangle$

Interfacial SOC Hamiltonian:

$$H_{\rm SO} = \delta(z)\left[f^R(x,y)\left(P_y\sigma_x - P_x\sigma_y\right) + f^D(x,y)\left(P_x\sigma_x - P_y\sigma_y\right)\right]$$

Momentum matrix elements

$$\begin{aligned} \langle L|\delta(z)f(x,y)P_x|L\rangle &= (1 - 0.24\cos(\varphi_{v,L}))\left[\lambda_x^L B_y + \mu_x^L B_z\right] \\ \langle L|\delta(z)f(x,y)P_y|L\rangle &= -(1 - 0.24\cos(\varphi_{v,L}))\left[\lambda_y^L B_x + \mu_y^L B_z\right] \\ \langle R|\delta(z)f(x,y)P_x|R\rangle &= (1 - 0.24\cos(\varphi_{v,R}))\left[\lambda_x^R B_y + \mu_x^R B_z\right] \\ \langle R|\delta(z)f(x,y)P_y|R\rangle &= -(1 - 0.24\cos(\varphi_{v,R}))\left[\lambda_y^R B_x + \mu_y^R B_z\right] \\ \langle R|\delta(z)f(x,y)P_x|R^*\rangle &= 0.24 * i\sin(\varphi_{v,R})\left[\lambda_x^R B_y + \mu_x^R B_z\right] \\ \langle R|\delta(z)f(x,y)P_y|R^*\rangle &= -0.24 * i\sin(\varphi_{v,R})\left[\lambda_y^R B_x + \mu_y^R B_z\right] \\ \langle R^*|\delta(z)f(x,y)P_x|R^*\rangle &= (1 + 0.24\cos(\varphi_{v,R}))\left[\lambda_x^R B_y + \mu_x^R B_z\right] \\ \langle R^*|\delta(z)f(x,y)P_y|R^*\rangle &= -(1 + 0.24\cos(\varphi_{v,R}))\left[\lambda_y^R B_x + \mu_y^R B_z\right] \end{aligned}$$

$\varphi_{v,L}$ = valley phase of left dot

$\varphi_{v,R}$ = valley phase of right dot

Factor of 0.24 comes from form factor approximation for Bloch functions

Measurement of Valley Splitting

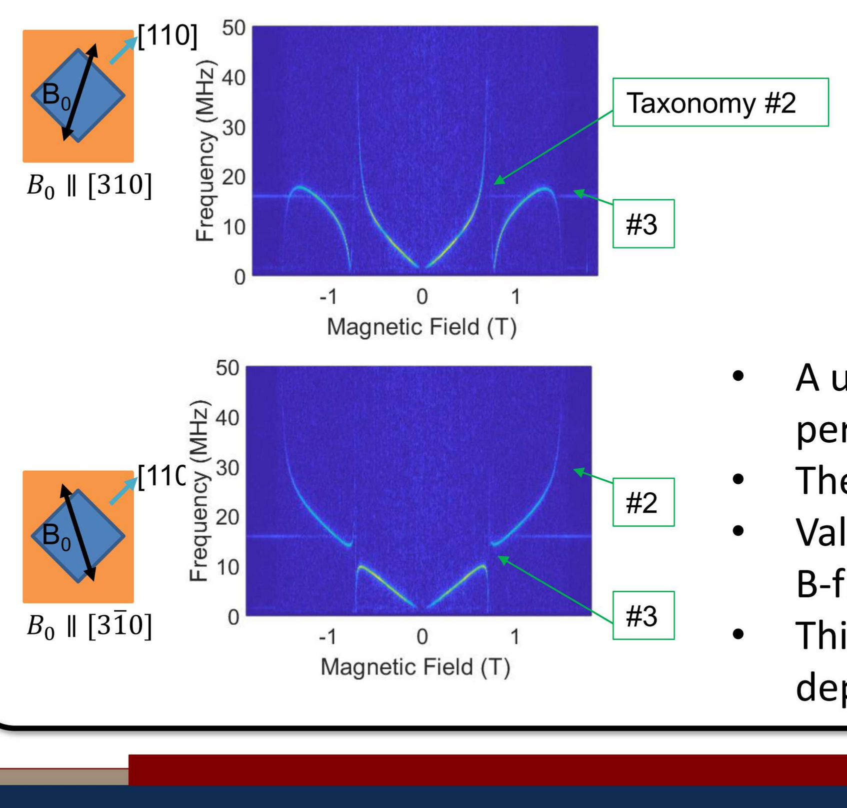

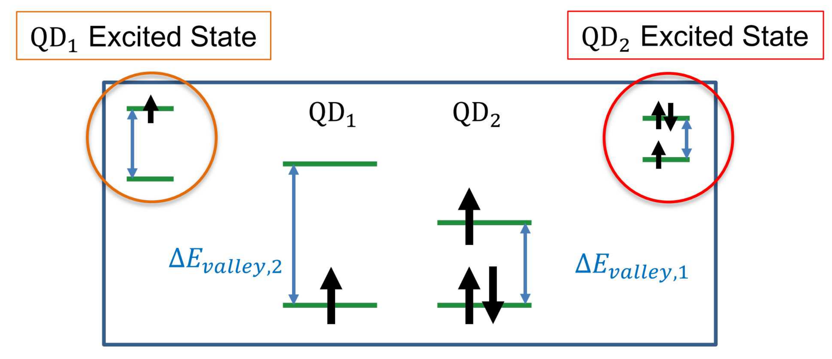

- A useful feature of this qubit operating mode is the ability to perform high-sensitivity measurements of valley splitting.
- The valley splitting sets the location of the quasi-divergence
- Valley splitting sensitivity is limited primarily by calibration of B-field and line width of the coherent rotation frequency
- This technique should be able to measure B-field dependence of valley splitting or at least tightly bound it

Summary

- Our MOS DQD singlet-triplet qubit exhibits a complex angular dependence as a function of B-field orientation
- Our model for intra- and inter-valley SOC captures all features of a complete angular dependence and points towards further insights into the nature of SOC at the Si/SiO_2 interface
- This approach also provides a means of measuring valley splitting with high precision

[1] Yang, et al. Nat. Comm. 4, 2069 (2013)
[2] Hao, et al. Nat. Comm. 5, 3860 (2014)
[3] Veldhorst, et al. Nat. Nano. 9, 981 (2014)
[4] Borjans, et al. PRA 11, 044063 (2019)
[5] Scarlino, et al. PRB 95, 165429 (2017)
[6] Corna, et al. npj Quant. Info 4:6 (2018)
[7] Huang, et al. PRB 95, 075403 (2017)
[8] Harvey-Collard, et al. PRL 122, 217702 (2019)
[9] Veldhorst, et al. PRB 92, 201401 (2015)
[10] Jock, et al. Nat. Comm. 9, 1768 (2018)
[11] Fogarty, et al. Nat. Comm. 9, 4370 (2018)
[12] Tanttu, et al. PRX 9, 021028 (2019)

NNSA National Nuclear Security Administration

U.S. DEPARTMENT OF ENERGY

This work was performed, in part, at the Center for Integrated Nanotechnologies, an Office of Science User Facility operated for the U.S. Department of Energy (DOE) Office of Science. Sandia National Laboratories is a multi-mission laboratory managed and operated by National Technology and Engineering Solutions of Sandia, LLC., a wholly owned subsidiary of Honeywell International, Inc., for the U.S. Department of Energy's National Nuclear Security Administration under contract DE-NA-0003525.

Sandia National Laboratories